JOURNAL OF MATERIALS SCIENCE 10 (1975) 2050–2061

Fracture mechanisms in glass-reinforced plastics

B. HARRIS, J. MORLEY
School of Applied Sciences, The University of Sussex, Falmer, Brighton, UK
D.C. PHILLIPS
Materials Development Division, AERE, Harwell, Didcot, Oxon, UK

Model glass fibre/polyester resin composites have been made in the form of double cantilever beams and the effect of a small number of fibres on quasi-static crack propagation has been studied by simultaneous plotting of load/deflection curves, measurements of crack length, and observation of the progress of fibre/resin debonding and fibre pull-out. By varying the condition of the fibre surface and the arrangement of the fibres to a limited extent and carrying out subsidiary experiments on single-fibre samples of identical character it has been possible to make direct measurements of all of the important parameters required for an analysis of the macroscopic behaviour in terms of established models of fibre/matrix interaction. Agreement between experimental and calculated fracture energies for these model composites is not highly satisfactory, but it seems clear that the fracture energy of grp is likely to be determined very largely by work done against friction between fibres and matrix after the debonding process has occurred. This conclusion opposes the currently-held view which attributes the large γ_F values of grp to the fibre/resin debonding mechanism.

1. Introduction

Interpretation of macroscopic fracture behaviour of composites with reference to the physics of fibre/matrix interaction is not at all straightforward. The physical parameters required must usually be obtained in separate model experiments for which the conditions may be quite different and unrelated to the real composite behaviour, or they may have to be deduced second-hand from visual observation of the composite fracture. We have tried to remove some of the uncertainty inherent in such correlations by carrying out controlled crack-growth experiments on resin samples containing only a few glass fibres. We have analysed their macroscopic behaviour in terms of the external work expended in breaking the samples and the apparent critical stress intensity parameter. Simultaneously we have studied microscopic failure events, clearly visible in these samples, monitoring progressive changes in the appearance of the glass/resin system during crack growth. Subsidiary experiments on single-fibre samples have also been carried out where necessary, but on specimens cut directly from identical composites. Control over the nature of the fibre surface and fibre strength was ensured by drawing the fibres individually, in the laboratory, immediately prior to casting them into the resin. In this way we have been able to make direct measurements of all of the important parameters needed for an analysis of the macroscopic behaviour in terms of established models of fibre/matrix interaction.

2. Experimental work

The composites were prepared as double cantilever beam samples similar to those used by McGarry and Mandell [1] with the dimensions shown in Fig. 1. The deep side slots were needed to obviate running-out of the crack, and the analysis we have used was that of Johnson and Radon [2] who give for the critical stress-intensity factor, K_{IC}, in plane

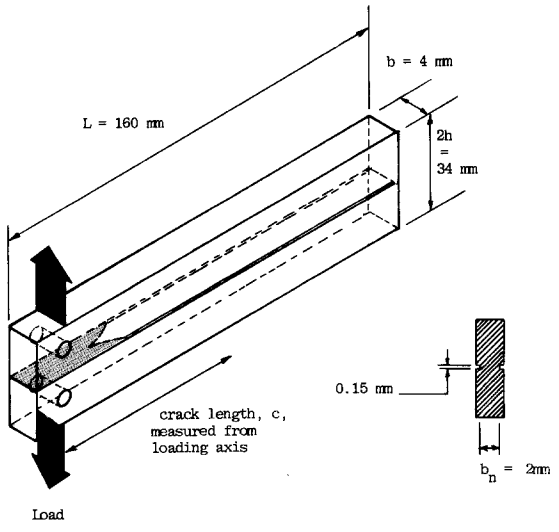

Figure 1 Shape and size of double cantilever beam specimens.

strain:

$$K_{IC} = \frac{3.46P(c/h + 0.7)}{[b b_n h(1 - \nu^2)]^{\frac{1}{2}}} \quad (1)$$

where P and c are the load and crack length corresponding to an increment of rapid crack growth, and ν is Poisson's ratio. The side grooves were cut with a fine rotary saw and the leading edge of the initial sawn notch was of the fish-tail shape advocated by Griffiths and Holloway [3]. We do not claim that the results we obtain can be regarded as conventional critical stress-intensity factors: we shall refer to our values of the parameter defined by Equation 1 simply as K' – a function of stress and crack length – and use these to compare the behaviour of different samples.

These samples were cut from plates made by casting catalysed polyester resin (BXL SR 17449) to fill one half of an open, horizontal plate mould and laying the fibres, spaced at about 12 mm intervals, onto the surface of this layer of resin after it had gelled. An equal quantity of the same resin mix, which had been temporarily refrigerated to retard gelation, was then cast into the top half of the mould and the sample was allowed to cure at room temperature. Test pieces were machined prior to post-curing while the resin retained slight ductility, and the samples were then post-cured for 16 h at 100° C. A plain resin sample and four plates containing glass fibres were prepared in this way. The fibres were drawn immediately before placing in the resin by heating a piece of soda glass rod to red heat and pulling the ends to full arm span. After a little practice it was possible to obtain uniform fibres about 0.25 mm in diameter sufficiently long to prepare a plate containing six fibres.

The first plate contained freshly-drawn fibres embedded in the resin within minutes of drawing. The second plate contained fibres that had been allowed to dry after immersion in a 5% solution in acetone of Union Carbide's A187 organo-silane coupling agent (γ-glycidoxypropylsilane). The third plate contained fibres which had been drawn once between finger and thumb prior to embedding and the fourth contained fibre damaged in the same way but lying at an angle of about 68° to the crack plane instead of perpendicular to it. The mean strength of the freshly-drawn fibres was 990 MN m^{-2} while that of the handled fibres was 580 MN m^{-2}. The mean diameter of fibres in each plate was established by polishing off one of the fractured faces of the plate and measuring each fibre. Basic experimental data relating to the four composite beams are shown in Table I.

Fracture tests were carried out quasi-statically in an Instron machine, the load being applied by turning the manual control to drive the servo

TABLE I Description of experimental composite materials

	Fibre surface condition	Fibre diameter d, (mm)	No. of fibres N	V_f
1	Freshly-drawn, clean fibres	0.253	6	9×10^{-4}
2	Fibres treated with A187 organosilane	0.268	5	8.5×10^{-4}
3	Fibres handled after drawing	0.231	6	7.6×10^{-4}
4	Handled fibres at 68° to crack plane	0.262	6	9.6×10^{-4}

The resin used was polyester BXL SR 17449, with MEK peroxide catalyst and cobalt naphthanate accelerator in the ratio 50 : 1 : 1 parts by weight.

system instead of driving the machine at constant cross-head speed. Small load increments could then easily be applied and loading stopped when any movement of the crack tip occurred. The sample was illuminated by polarized light so that the position of the crack front and the extent of fibre/resin debonding could be seen through a travelling microscope. Measurement of the load, P, the crack length, c, and the length, y, of the debonded region in each fibre were recorded during the test, and after a sample was completely fractured the lengths, l_p, of all fibre ends that that had pulled out of the matrix were determined.

In subsidiary experiments, samples containing single fibres were cut from unbroken plates and tensile tested. These single fibre samples, which already contained side grooves, were cut on the remaining two sides so as to leave only a small amount of resin surrounding the fibre. Before testing, the samples were twisted slightly so that the remaining resin cracked without severing the fibre. This was easily done in samples containing silane-treated or handled fibres, but was difficult in those containing clean fibres. In the latter, the crack most frequently ran straight through both resin and fibre with little debonding. The load–deflection curves obtained by loading these precracked samples to fracture in tension were used to determine the initial frictional force and the actual pull-out work.

3. Experimental results

3.1. Fracture work and fracture toughness

Complete load–deflection curves for the four composite samples are shown in Fig. 2. There are two obvious distinguishing features: (i) the total energy required to break the samples containing silane-coated fibres and misoriented fibres is lower than that for either of the other two; (ii) the curve for the sample containing handled fibres shows two distinct components – the large drops in load are associated with increments of crack growth, but between these events there are many smaller load drops and recoveries which contribute substantially to the high fracture energy. These smaller drops have since been shown quite unambiguously to be associated with sudden increments of debonding and fibre pull-out, the latter occurring by a discontinuous stick-slip mechanism [4].

Values of K' were calculated for each increment of crack growth. In order to compensate for different numbers of fibres and different mean diameters in the four composite samples (Table I), these values of K' were all normalized to a notional "volume fraction" of 0.0009 by multiplying by $0.0009/[V_f\,(\text{actual})]$. The normalized values are plotted as a function of crack length, together with results for the plain resin, in Fig. 3. Although the K' values for all of the composites rise above the stable resin value (about $0.5\,\text{MN}\,\text{m}^{-3/2}$), the curves for silane-treated and misoriented fibre

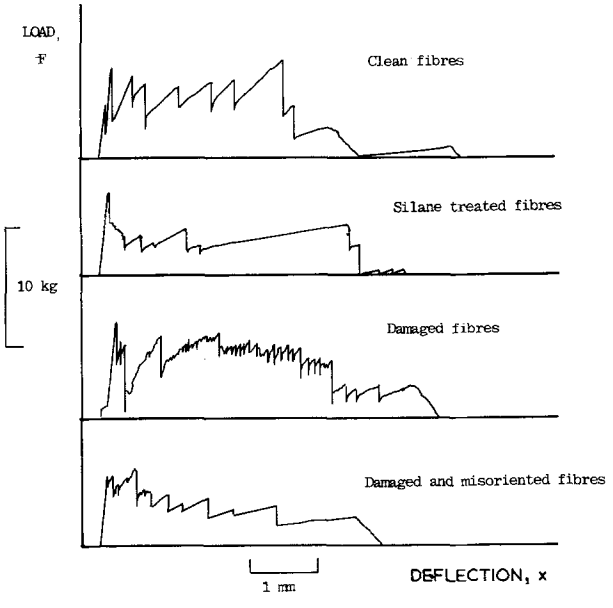

Figure 2 Load versus deflection (or crack-opening displacement) curves for quasi-static fracture of DCB composite samples containing (a) clean fibres, (b) silane coated fibres, (c) fibres damaged by handling, and (d) damaged fibres at an angle of 68° to the crack plane.

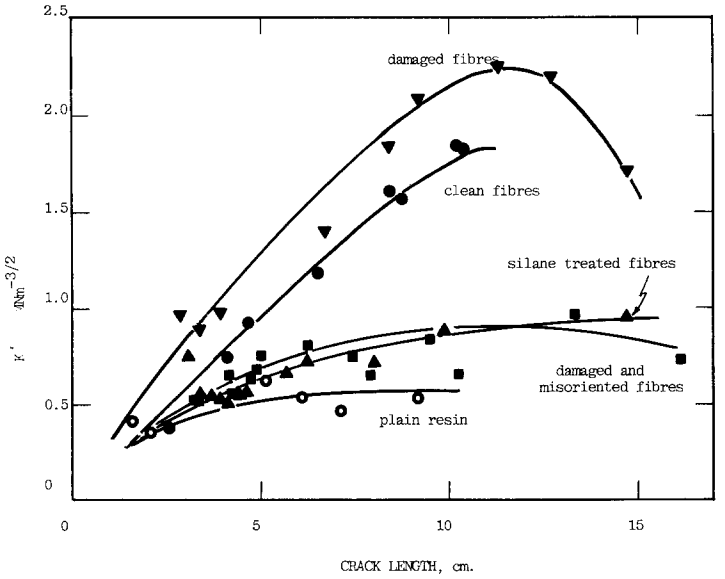

Figure 3 Apparent critical stress intensity factor, K', as a function of crack length for plain polyester resin and four composite beams. The fibre treatments are the same as those represented in Figure 2 and Table I.

composites rise to maximum values less than twice that of the resin, whereas the other two curves rise to between three and four times this level. Mean values of K' were converted to the equivalent fracture energies, γ_F, on the assumption that the fracture mechanics relationship.

$$K_{IC}^2 \approx 2(1-\nu^2)E\gamma_F \text{ (plane strain)} \quad (2)$$

also holds for K'. The value of E used was that for the resin since there was so little reinforcement, and the values obtained are shown, together with the areas under the curves of Fig. 2, in Table II. The integration values are divided by the total crack surface area to allow comparison with conventional surface fracture energies. The agreement between the two estimates of γ_F is good for samples 1 and 3, but for samples 2 and 4 the result derived from fracture mechanics is only about half that measured directly. The ranking is the same in both cases, however.

3.2. Fibre debonding and fibre pull-out

During crack growth, resin cracks would sometimes stop in the regions between fibres and they were often, but not invariably, halted by fibres. The stopping of a crack at a fibre and the onset of fibre/resin debonding usually appeared to occur simultaneously, but during subsequent reloading, further debonding would often occur before the crack could grow past the fibre. In some cases two or three fibres would remain unbroken behind the crack front and the debonding process would continue until a fibre broke. Fibres often fractured at the crack plane even after extensive debonding, but fracture inside the resin and fibre pull-out also occurred. The samples were illuminated by trans-

TABLE II Measured and derived fracture parameters

Sample		Mean K' ($MN\,m^{-3/2}$) (±0.05)	Mean γ_F (derived from $\bar{K}'$ ($J\,m^{-2}$) (± 5)	γ_F (graphical value) ($J\,m^{-2}$) (± 5)
-	Plain resin	0.5	40	-
1	Clean fibres	1.3	280	250
2	Silane coated fibres	0.7	90	180
3	Handled fibres	1.6	400	370
4	Handled fibres, angled	0.7	90	160

All values of K' and γ_F for composites are normalised to $V_f = 0.0009$.

TABLE III Fibre/resin debonding and fibre pull-out

Sample	Mean debond length* $\bar{y}$ (mm)	Max. value of debond length* (mean for all fibres) y_{max} (mm)	Fibre pull-out length; mean for all fibres, l_p (mm)	$y_{max}/\bar{l}_p$
1	6.3	9.8	1.07	9.2
2	10.7	12.8	1.35	9.5
3	28	34	3.2	10.6
4	14	14	0	

* The debond length, y, is the total debonding per fibre and is measured on both sides of the crack plane.

mitted polarized light during testing and the position of the crack front, the extent of debonding, and the stress transmitted between fibre and resin during fibre pull-out were made clearly visible by stress birefringence. The debonded lengths at each fibre were measured for each increment of crack growth and the mean and maximum values are recorded, together with mean pull-out lengths, in Table III. When attempts are made to analyse the fracture behaviour of composites, the value of the fibre critical length, l_c, is usually required and in the absence of a direct determination an estimate is often made from the appearance of the fracture surface. The "mean" length of fibre pull-outs, $\bar{l}_p$, which can be roughly estimated from scanning electron micrographs, is assumed to be half the maximum possible pull-out length, and this should, in turn, be equal to $l_c/2$, so that $l_c \approx 4\bar{l}_p$. It is also often assumed that the total debond length is of the order of l_c, whence $y \approx 4\bar{l}_p$. The results in Table III show, however, that for those composites where debonding and pull-out occurred together, the ratio of (maximum debond length/(mean pull-out length) is about 10. When the fibres do not lie normal to the crack plane there is no pull-out as might be expected, and the extent of debonding is much smaller than when the fibres are arranged vertically.

3.3. The work of fibre pull-out and the friction force

When single fibre samples were loaded in tension the load–deflection curves showed two characteristic regions. The initial, steeply rising portion (Fig. 4) is associated with elastic deformation of the fibre and a gradual change in the stress distribution between resin and fibre as debonding occurs. When the fibre breaks the load drops rapidly but if, as is frequently the case, the fracture is within the resin, the resin re-asserts its grip on the fibre and the load may be maintained at a substantial level, P_μ. The high level of this friction load and the amount of work required subsequently to withdraw the broken fibre end from the resin conflict directly with the familiar assertion [5, 6] that the pull-out work can be ignored in glass-reinforced plastics. We also note that whereas the pull-out load on a damaged (handled) fibre falls fairly smoothly as pull-out progresses, implying a reasonably constant value of the interfacial friction stress, it increases intially during pull-out of a silane-treated fibre. The curious behaviour obser-

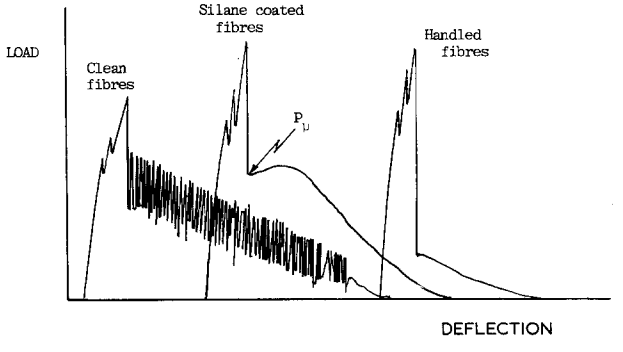

Figure 4 Typical load–deflection curves for pull-out of single glass fibres from blocks of polyester resin. The actual load levels are not comparable because the lengths of fibre ends being pulled out were different. But the relative areas of the initial (elastic stretching, debonding and fracture) and secondary (pull-out) portions may be compared.

TABLE IV Work of fibre pull-out and interfacial friction stress (single fibre samples)

Fibre condition	Initial friction stress, τ_i ($MN\,m^{-2}$)	Effective friction stress, τ_{eff} ($MN\,m^{-2}$)	Critical length* l_c (mm)	Work of fibre pull-out, w_p ($kJ\,m^{-2}$) (of fibre surface)
Clean fibres	6.0	3.2	21	8.1
Silane coating	8.6	13.4	15	13.7
Damaged fibres	5.3	4.0	13	2.7

* from $l_c/d = \sigma_f/2\tau_i$.

ved when clean fibres are pulled out indicates a stick-slip friction mechanism, but there again the mean value of the load falls smoothly during the pull-out process.

The work of pulling out a fibre end of length l_p measured directly from the load–deflection graph is

$$w_p = \int_0^{l_p} P\,dx.$$

Although the interfacial friction stress apparently does not always remain constant during pull-out, we can calculate an effective friction stress, τ_{eff}, by assuming that this stress does work $\frac{1}{2}\tau\pi d l_p^2$ which is equal to w_p and

$$\tau_{eff} = \frac{2w_p}{\pi d l_p^2}.$$

The value of the interfacial friction stress at the start of pull-out immediately following fibre fracture is

$$\tau_i = \frac{P_\mu}{\pi d l_p}$$

and values of τ_{eff} and τ_i for composites showing pull-out may be compared in Table IV where the actual work of fibre pull-out, w_p, related to the surface area of the pulled-out end, is also recorded. For untreated fibres and damaged fibres the initial level of interfacial shear stress is not maintained during pull-out, contrary to what is commonly assumed, whereas if the fibres are silane treated the shear stress increases during pull-out.

The similarity between the three values of τ_i is not so surprising if we assume that the principal effect of surface treatments (including handling) is to alter the initial tensile and shear *debonding* characteristics rather than alter the ordinary friction coefficient between sliding glass and resin surfaces. Weakening of the fibres is immaterial in this respect. Once pulling out starts it is then still not totally unexpected that the friction force should fall slightly if during the pull-out process, any residual secondary adhesive bonds are broken or any small asperities on the glass or resin surfaces are smoothed out. These explanations would be reasonable for samples 1 and 3 where no "extra" material is interposed between fibre and resin. A silane coating, on the other hand, is likely to be less brittle than the resin and would in any case cover the glass only imperfectly [7]. If small "rubbery" islands could become detached from the glass and resin during pull-out they could easily deform as they are dragged along and increase the effective friction coefficient.

3.4. The critical transfer length

Since in all our experiments where debonding and pull-out occur together, $y_{max} \approx 10 l_p$, "critical lengths" calculated from y_{max} and $\bar{l}_p$ would be quite different. From $\bar{l}_p$ values, fibres in samples 1, 2 and 3 should have critical lengths of 4.3, 5.4 and 13 mm respectively, whereas the equivalent values from y_{max} are about 10, 13 and 34 mm. However, these results are completely at variance with other published values such as those of Carswell and Lockhart [8] and Hancock and Cuthbertson [9], and the usual value reported for (presumably) clean fibres in polyester or epoxy resin is about 13 mm. If data from the single fibre pull-out experiments are used to determine l_c, and measured values of fibre strength and initial friction force are substituted in the relationship

$$l_c/d = \sigma_f/2\tau$$

we find that l_c is 21, 15 and 13 mm for the same three samples (Table IV). The value for clean fibres

is rather high, but the other two are acceptable, and none bears any convincing resemblance to those derived from $\bar{l}_p$ and y_{max}.

4. Discussion

The measured values of K' increase with crack length in composite samples, and at the point when the final catastrophic propagation of the crack occurs the crack faces may still be tied together by several unbroken fibres. Since the sample can then still apparently have a non-zero K' value because the load on the sample is borne entirely by unbroken fibres which are being pulled out, the crack having passed completely through the resin, the use of the stress intensity concept is clearly suspect. Furthermore, since so few fibres are involved the failure of only one fibre at a statistically low load could thus make a significant difference to the last few measurements of K' with the result that a value of γ_F for such a sample, obtained from the mean K' as in Table II, could quite easily fall well below the integrated work of fracture. This would presumably account for the discrepancies between the two values of γ_F for samples 2 and 4 in Table II.

An additional consequence is that the maximum values of K' measured on composites containing fresh fibres and damaged fibres may not be truly representative of the maximum possible crack resistance obtainable in longer samples (or in real composites). Nevertheless, the differences in behaviour resulting from the various fibre and interface conditions are significant. They corroborate the observation of Outwater [10] that preserving the cleanliness of fibres and using coupling agents during the manufacture of grp are not necessarily beneficial for applications where toughness rather than strength is the critical design requirement. The presence of a minute quantity (< 0.1 vol. %) of "dirty" fibre increases the fracture toughness of the base resin by a factor of four. Scaling up linearly to compositions typical of commerical grp composites ($V_f \sim 0.70$) implies multiplying by about 10^3, giving an extrapolated value of about $2\,GN\,m^{-3/2}$ for K'. Values reported for real composites are much lower than this, however, and the work of Owen and Rose [11], for example, indicates that 10 or 20 would be a more reasonable multiplying factor.

Outwater and Murphy [5] have shown how Griffith's use [12] of the first law of thermodynamics to describe the fracture of brittle solids may be extended to fibre-reinforced composites. In the Appendix we expand Outwater's treatment somewhat in order specifically to consider effects which he considered negligible and to permit the correlation of experimental and theoretical results. From this we take as the basis for our discussion the final Equation A10:

$$\gamma_F = \frac{1}{2A}\int_0^{\text{failure}} F\,dx = \frac{w_2}{2A} + \frac{w_3}{2A} + \frac{w_4}{2A} + \gamma_{s,m} + \gamma_{s,i}. \quad \text{(A10)}$$

γ_F is the total work of fracture of the composite, measured directly as $\int_0^{\text{failure}} F\,dx$, the integrated load–deflection curves; w_2 is the elastic energy stored in the fibres at failure (debonding energy); w_3 is the post-debonding friction work; w_4 is the pull-out friction work; $\gamma_{s,i}$ is the "surface" energy of interface created during debonding; and $\gamma_{s,m}$ is the constant matrix surface fracture work, $42\,J\,m^{-2}$. The calculated work and energy terms in equation A10 together with the summation of the R.H.S., are shown in Table V. The level of agreement is not particularly good except for sample 3. It seems likely that the discrepancy in the case of sample 4 is partly attributable to the fact that when fibres are at an angle to the crack plane the resin fracture face, normally smooth, flat and mirror-like, becomes highly irregular. This appears

TABLE V Summary of calculated and measured fracture energy values

Sample	Debond energy, $w_2/2A$ ($J\,m^{-2}$)	Post-debond friction work, $w_3/2A$ ($J\,m^{-2}$)	Pull-out friction work, $w_4/2A$ ($J\,m^{-2}$)	Matrix fracture energy, $\gamma_{s,m}$ ($J\,m^{-2}$)	Interface fracture energy, $\gamma_{s,i}$ ($J\,m^{-2}$)	Total estimated fracture work (Equation A10) ($J\,m^{-2}$)	Measured fracture work, γ_F ($J\,m^{-2}$)
1	31	29	62	42	4	169	253
2	38	63	117	42	4	264	167
3	32	160	56	42	11	301	312
4	16	31		42	5	94	168

to be because the crack tries to run normal to the fibres and as a result passes into the thicker parts of the sample each time it moves past a fibre. Perhaps the overall lack of agreement is not surprising when we consider that only five or six fibres are involved in each composite and there is a strong possibility that none will break exactly at the statistical mean values used in the calculations. What is important, however, is the relative magnitude of the separate contributions to the total fracture energy. It is clear the two friction terms dominate all other components, and friction clearly plays a larger part in determining work of fracture than has hitherto been implied by Outwater's analyses. Although several determinations of the interfacial bond shear strength have been made, there is little measure of agreement between them. For single fibre pull-out tests Norman *et al.* [13] report a value of 20.6 $MN\,m^{-2}$ for polyester/glass and this agrees with Hancock and Cuthbertson's value of $22\,MN\,m^{-2}$ for epoxy/glass at low V_f. Hancock and Cuthbertson [9] show, however, that the value can be as low as half this in normal composites. Broutman [6] reports values between 4.2 and $6.9\,MN\,m^{-2}$ for the shear debond stress and observes that silane coatings do not increase the bond strength. On the other hand he shows that silane coatings can increase the tensile debond stress from 5.2 to $8.4\,MN\,m^{-2}$. Murphy and Outwater [5] showed that the debond energy, w_2, measured in single fibre shear experiments (G_{IIc} in their notation) could be halved either by handling the fibres or by applying conventional surface treatments, a conclusion not apparently corroborated by our own results. They also state that the post-debond friction force in glass/epoxy systems was only $1.4\,MN\,m^{-2}$. Laws *et al.* [14] point out that except for very short fibre lengths, the composite strength and toughness would be more effectively improved by increasing the interfacial friction stress, static or dynamic, than increasing the interfacial shear bond strength. This is certainly in agreement with our own findings.

In a series of experiments similar to our own, Mandell and McGarry [1] used bundles of glass yarns in their cantilever beam samples. Some of their conclusions may be compared with ours, as follows.

(1) They suggest that toughness increases if the fibre strength is increased. In our experiments the opposite has occurred because when glass fibres were weakened by handling there was a concomitant change in pull-out length because the interfacial friction force remained roughly the same.

(2) Work of fracture increases if the extent of debonding increases. Fig. 3 shows a similar effect: in sample 3 with fibres damaged by handling the fibres were debonded to the full extent of the sample height, and this sample has the highest toughness. Even in this case, however, the fibres were not pulled out over their whole debond length. The increases in toughness with crack length illustrated in Fig. 3 also suggest a relationship between toughness and the length of debonded fibre. If the individual values of K' at each crack length are converted to γ_F values, as described earlier, and these are then divided by the total length of debonded fibre, Σy, measured directly from the sample during the test, the ratio $\gamma_F/\Sigma y$ becomes constant after stable crack growth conditions have been established although, as Fig. 5 shows, the proportionality constant depends on fibre and surface conditions. Since two of the terms on the R.H.S. of Equation 3 are

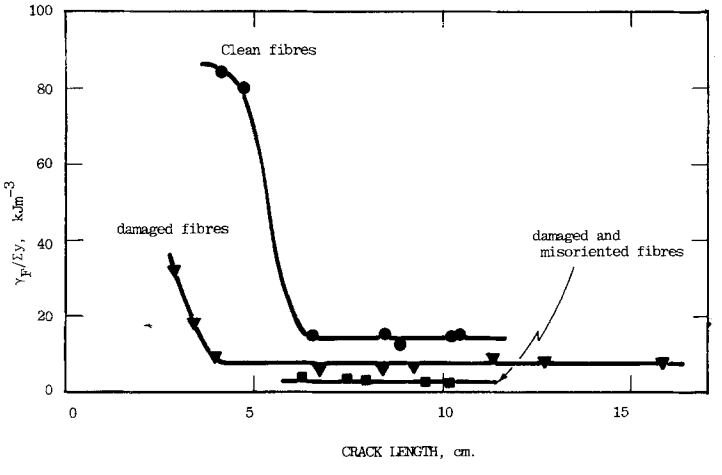

Figure 5 The apparently linear relationship between the fracture energy, γ_F, and the total length of debonded fibre is shown here by the constancy of the ratio $\gamma_F/\Sigma y$ as a function of crack length after an initial rapid drop.

roughly proportional to y and two are proportional to y^2, this result is perhaps not surprising.

(3) Toughness increases with fibre volume fraction. This is expected since only one term in Equation 3 is independent of the number of fibres. But it is not clear what form the relationship will take since we cannot easily predict how the interface friction stress and the fibre critical length will vary as the stress systems in the neighbourhood of each fibre begin to interact.

(4) No significant effect of fibre orientation on either toughness or debond length was observed for yarns lying up to 60° from the perpendicular. This is clearly at variance with our own results and the most likely explanation is that our thicker fibres are much more rigid and, therefore, able to sustain a much smaller degree of curvature before breaking at the crack face. Not only is there then no fibre pull-out but the extent of debonding is also reduced since the fibres fail under smaller tensile loads when there is a large added bending component. There are obvious implications of this result for the users of composites containing thick boron fibres as opposed to the usual very fine glass and carbon fibres, and for users of laminated or chopped fibre composites.

5. Conclusion

It has been possible to show, by studying the propagation of cracks in model composite beams and simultaneously measuring all of the important reinforcement parameters, that the fracture energy of glass reinforced plastics is likely to be determined very largely by work done against friction between fibres and matrix after the debonding process has occurred. A comparison between experimental and calculated values of fracture energy for a number of different fibre surface treatments gives only a modest level of agreement, possibly as a result of the fact that the number of fibres in each composite was to small to permit the use of statistical mean strengths, pull-out lengths, debond lengths, etc.

6. Appendix: Estimation of contributions to total fracture energy

With the convention that work done *by* a system is positive, the first law of thermodynamics in its most general form [15] is

$$\mathrm{d}U = \mathrm{d}Q - \sum_i \Psi \mathrm{d}\psi_i \qquad \text{(A1)}$$

where for our particular case $\Psi \mathrm{d}\psi$ includes all work terms of the form $f\mathrm{d}x$ (elastic extension) and $\gamma \mathrm{d}A$ ("surface" energy).

The highest fracture energy measured was equivalent to about 0.5 J in terms of work expended on the sample. If the sample were thermally isolated the irreversible conversion of this work to heat in a 30 g sample of specific heat $2000\,\mathrm{J\,kg^{-1}\,K^{-1}}$ would raise its temperature by about 0.01° C. It is most unlikely that in a quasi-static experiment a temperature rise as high as this could have occurred in the sample as a whole, and even in the vicinity of the crack tip substantial heating was probably absent. We shall tentatively assume, therefore, that $\mathrm{d}Q = 0$. The resin matrix is loaded elastically during the experiment and its internal (potential) energy is initially increased, but subsequently the sample is completely unloaded by the slow propagation of the crack. The thermodynamic state of an element of resin remote from the crack face is, therefore, identical before and after the sample is broken, and since the surface fracture work is to be treated as distinct from internal energy the recoverable elastic energy does not enter into the equation and $\mathrm{d}U = 0$. Equation A1 is then

$$\sum_i \Psi \mathrm{d}\psi_i = 0$$

or

$$\sum f\mathrm{d}x + \sum \gamma \mathrm{d}A = 0. \qquad \text{(A2)}$$

Each of these terms consists of several components. $\Sigma f\mathrm{d}x$ includes work done *on* the system by external forces, the work done *by* the system against friction between resin and fibres, and the irrecoverable work done *by* the system in loading up debonded fibres to their fracture point. The total work done by the applied force, F, on the system boundary (defined here so as to contain the specimen only) is the area under the load–deflection curves of Fig. 2 and is, therefore,

$$w_1 = -\int_0^{\text{failure}} F\mathrm{d}x. \qquad \text{(A3)}$$

As the crack passes through the beam, lateral tensile forces at the tip initiate fibre/resin debonding which spreads in discontinuous steps along the fibre. As it debonds the fibre is directly loaded over an unsupported length until a critical flaw within this debonded length initiates fracture. This is an uncontrolled process and the stored elastic energy in the fibre at failure, which is far in excess of the fibre surface energy, is released irrecoverably as kinetic, acoustic and thermal energy. The energy, w_2, to load the fibre to failure over the

debonded length is called the debonding energy [10]. After debonding and fibre fracture have occurred, the fibre and resin will have moved relative to each other. If the fibre is still gripped by the resin, and our experiments show that it is, work must, therefore, have been done against this interfacial friction. This post-debonding friction work, w_3, is easily distinguished from the pull-out friction work, w_4, that is now required to withdraw the broken fibre end from the resin, also against interfacial friction. The sum $\Sigma f dx$ is, therefore,

$$\sum f dx = -w_1 + w_2 + w_3 + w_4. \quad \text{(A4)}$$

This net work serves to create new surfaces and interfaces and the term $\Sigma \gamma dA$ is therefore the sum of three separate contributions from the resin, $\gamma_{s,m}$, the fibres, $\gamma_{s,f}$, and the new interfaces formed by the debonding process, $\gamma_{s,i}$. Outwater represents this as a debonding energy, G_{IIC}, which has the character of a strain energy release rate for mode II (shear) crack propagation along the interface. The energy balance equation is thus:

$$\int_0^{\text{failure}} F dx = w_2 + w_3 + w_4 + \gamma_{s,f} A_f + \gamma_{s,m} A_m + \gamma_{s,i} A_i \quad \text{(A5)}$$

where A_f, A_m, A_i are the fracture surface areas of fibres and matrix, and the area of new interface.

We can exclude the kinetic energy of separation of the resin crack faces since this was a quasi-static experiment, and we ignore the very small kinetic energy term for the fibres. There could also be a non-zero stored elastic energy term were there any residual stresses between the fibres and resin after total fracture or if cracking has altered the balance of any residual stresses set up by the curing contraction. However, there was no evidence of such residual stresses in terms of birefringence either before or after fracture, and we therefore ignore them. In order to obtain dimensionally and physically comparable results, all energy measurements and estimates are normalised by dividing by the total surface area of crack (two faces) produced during the experiment. Each energy or work term can then be directly compared with conventional fracture surface energies, γ_s, and with the work of fracture values, $\gamma_F = (1/2A) \int_0^{\text{failure}} F dx$, in Table II. We now attempt to estimate the terms on the R.H.S. of Equation A5:

$$\gamma_F = \frac{1}{2A}(w_2 + w_3 + w_4 + \gamma_{s,f} \cdot A_f + \gamma_{s,m} A_m + \gamma_{s,i} A_i) \quad \text{(A6)}$$

6.1. Debonding energy [10, 16]

If a fibre debonds to a total distance $y_{max}/2$ on each side of the crack face, the stored elastic energy released when it breaks is

$$w_2 = \tfrac{1}{2}(\sigma_f^2/E)(\text{volume}) = \tfrac{1}{2}(\sigma_f^2/E) \cdot (\pi d^2/4) y_{max},$$

and if N fibre break

$$\frac{w_2}{2A} = \frac{N \pi d^2 \sigma_f^2 y_{max}}{16 A E_f}. \quad \text{(A7)}$$

This must, in fact, be an overestimate since it assumes that the fibre/resin interfacial shear strength falls to zero after debonding and our results clearly show that this assumption is untenable (see, for example, Kelly [17]. Outwater's own determinations of the parameter G_{IIC} were made by compressing prismatic resin samples containing single fibres and it seems likely that his experiment introduces a substantial tensile debonding component whereas in a conventional mode I fracture there will be a large shear debonding force. It is by no means certain, then, despite the fact that many of our observations mirror those of Outwater, that the values of G_{IIC} he uses are relevant to our analysis. We have therefore adopted Outwater's Equation (A7) as an upper bound instead of using his measured G_{IIC} values. If Equation A7 is modified so as to refer to the debonded surface area of a single fibre the debonding work becomes

$$w_d = \frac{w_2}{\pi d y_{max}} = \frac{\sigma_f^2 d}{8 E_f}$$

which is given by Outwater as an upper bound to the debonding energy. Outwater's measured value of w_d (or G_{IIC} max) is $4\,\text{KJ m}^{-2}$ for clean glass/epoxy, which is about ten times our own value for composites 1 and 2.

6.2. Post-debond friction work [17, 18]

The total work expended will result from the action of the interfacial friction force over a distance equal to the differential displacement of fibre and resin. Kelly suggested that this distance is roughly the product of the debonded length and the differential failure strain, $y_{max} \Delta\epsilon$. But in view of the relatively high rigidity of the matrix resin (or the surrounding composite in a real material) when compared with that of a single fibre, and the fact that the brittle resin crack propagates in any case at very low strains it is more likely that a better estimate is simply $y_{max} \times$ (fibre failure

strain). If the *initial* friction force, $\tau_i \pi d(y_{max}/2)$, acts in each direction from the crack face over a distance $\sigma_f(y_{max}/2)$, the work is

$$w_3 = \frac{2\tau_i \pi d y_{max}}{2} \cdot \frac{\epsilon_f y_{max}}{2} \quad \text{per fibre.}$$

For a composite containing N fibres

$$\frac{w_3}{2A} = \frac{N\tau_i \pi d y_{max}^2 \epsilon_f}{4A}. \tag{A8}$$

The relevant values of ϵ_f for clean and damaged fibres are found from known strength and modulus data to be 0.014 and 0.008 respectively.

6.3. Work of fibre pull-out [19, 20]

When a fibre end of length x is pulled from the matrix, the friction force, $\tau_{eff}\pi d(x/2)$ acts over the distance x to do work $\frac{1}{2}\tau_{eff}\pi d x^2$. Since x is normally considered to vary between $l_c/2$ and 0 in the average composite, the mean work done in pulling N fibres out to a maximum distance $l_c/2$, referred to the crack surface area, is

$$w_4 = \frac{N\pi d\tau_{eff}}{2} \frac{\int_0^{l_c/2} x^2 dx}{\int_0^{l_c/2} dx}$$

i.e.

$$\frac{w_4}{2A} = \frac{N\pi d\tau_{eff}\pi d l_c^2}{24A} \tag{A9}$$

However, since we have measured the work of pull-out, w_p; and the mean pull-out length, $\bar{l}_p$, is simply the total length of pulled-out fibre divided by the number of fibres in the composite, we can write

$$\frac{w_4}{2A} = \frac{N w_p \pi d \bar{l}_p}{2A}. \tag{A9}$$

This avoids the complication that we have already discussed that the mean pull-out length is not equal to $l_c/4$ except for sample 3.

6.4. Fibre surface energy

For an ideal brittle solid like glass the fracture surface work is of the order of only 5 J m^{-2}. Distributed over the total fracture area this would be minutely small and $\gamma_{s,f}$ will, therefore, be neglected.

6.5. Matrix surface energy

The appropriate value of $\gamma_{s,m}$ is 42 J m^{-2} which is the fracture surface work of the resin obtained from our measured values of K' and Equation 2 (Table II).

6.6. Interface surface energy

This is the difference in thermodynamic surface energy between the two states – fibre wetted by resin; and fibre and matrix surfaces separated by an air film: it is obtained from the work of adhesion. Marston *et al.* [16] have had some success in accounting for the fracture energies of glass, carbon- and boron-reinforced epoxy resins by associating a surface energy term with the actual debonded surface area although in the absence of measured $\gamma_{s,i}$ values they assumed that the $\gamma_{s,i}$ would not be very different from $\gamma_{s,m}$. It may be that $(\gamma_{s,m} + \gamma_{s,f})$ would be a more realistic estimate (~ 50 J m^{-2}), but in our case the energy $\gamma_{s,i}$ related to the sample cross-sectional area

$$\frac{N\pi d y_{max}\gamma_{s,i}}{2A}$$

is still a very small quantity, even for sample 3 with the largest debond lengths, because there are so few fibres.

From the foregoing, Equation A6 can now be reduced to

$$\gamma_F = \frac{N\pi d^2\sigma_f^2 y_{max}}{16AE_f} + \frac{N\tau_i \pi d y_{max}^2 \epsilon_f}{4A} + \frac{N w_p \pi d \bar{l}_p}{2A} + \frac{N\pi d y_{max}\gamma_{s,i}}{2A} + \gamma_{s,m}. \tag{A10}$$

References

1. F. J. McGARRY and J. F. MANDELL, 27th Annual Technical Conference of the Reinforced Plastics/Composites Institute of the Society of the Plastics Industry, paper 9-A (1972).
2. F. A. JOHNSON and J. C. RADON, *Eng. Fract. Mechs.* 4 (1972) 555.
3. R. GRIFFITHS and D. G. HOLLOWAY, *J. Mater. Sci.* 5 (1970) 302.
4. A. ANKARA, Sussex University, private communication.
5. M. C. MURPHY and J. O. OUTWATER, 28th Annual Technical Conference, Reinforced Plastics/Composites Institute of SPI, paper 17-A (1973); also 24th Annual Technical Conference, paper 11c (1969).
6. L. J. BROUTMAN, in "Modern Composite materials", edited by L. J. Broutman and R. H. Krock (Addison-Wesley, Reading, Mass., 1967) p. 337.
7. O. K. JOHANNSON, F. O. STARK, G. E. VOGEL, R. M. FLEISCHMANN and O.L. FLANINGAM, in " Fundamental Aspects of Fibre Reinforced Plastic Composites", edited by R. T. Schwartz and H. S. Schwartz (Interscience, New York, 1968) p. 199.
8. W. S. CARSWELL and A. H. LOCKHART, unpublished internal report, N.E.L., East Kilbride.

9. P. HANCOCK and R. C. CUTHBERTSON, *J. Mater. Sci.* **5** (1970) 762.
10. J. O. OUTWATER and M. C. MURPHY, *Modern Plastics* **7** (1970) 160; see also *J. Adhesion* **2** (1970) 242.
11. M. J. OWEN and R. G. ROSE, *J. Phys. D Appl. Phys.* **6** (1973) 42.
12. A. A. GRIFFITH, *Phil. Trans. Roy. Soc.* **A221** (1921) 163.
13. R. H. NORMAN, D. I. JAMES and G. M. GALE *Chem. Eng.* October (1964) 243.
14. V. LAWS, P. LAWRENCE and R. W. NURSE, *J. Phys. D Appl. Phys.* **6** (1973), 523.
15. A. B. PIPPARD, "Classical Thermodynamics" (Cambridge U.P. 1961).
16. T. U. MARSTON, A. G. ATKINS and D. K. FELBECK, *J. Mater. Sci.* **9** (1974) 447.
17. A. KELLY, *Proc. Roy. Soc.* **A319** (1970) 95.
18. M. R. PIGGOTT, *Acta Met.* **14** (1966) 1429.
19. A. KELLY, "Strong Solids" (Oxford U.P., 1966) p. 161.
20. A. H. COTTRELL, *Proc. Roy. Soc.* **A282** (1964) 2.

Received 22 April and accepted 20 May 1975.